THE AMERICAN SOCIETY OF MECHANICAL ENGINEERS
345 E. 47 St., New York, N.Y. 10017

89-GT-55

Development of the Tip-Leakage Flow Downstream of a Planar Cascade of Turbine Blades: Vorticity Field

M. YARAS* and S. A. SJOLANDER**

Department of Mechanical and Aeronautical Engineering
Carleton University
Ottawa, Ontario
Canada K1S 5B6

ABSTRACT

The paper presents detailed measurements of the tip-leakage flow emerging from a planar cascade of turbine blades. Four clearances of from 1.5 to 5.5 percent of the blade chord are considered. Measurements were made at the trailing edge plane, and at two main planes 1.0 and 1.56 axial chord lengths downstream of the cascade. The results give insight into several aspects of the leakage flow including: the size and strength of the leakage vortex in relation to the size of the tip gap and the bound circulation of the blade; and the evolution of the components of vorticity as the vortex diffuses laterally downstream of the blade row. The vortex was found to have largely completed its roll-up into a nearly axisymmetric structure even at the trailing edge of the cascade. As a result, it was found that the vortex could be modelled surprisingly well with a simple model based on the diffusion of a line vortex.

NOMENCLATURE

a_s	=	Squire's eddy viscosity constant (Eqn. 8)
A	=	area
c	=	blade chord length
c_x	=	blade axial chord length
C_P	=	$(P - P_{CL})/(1/2\rho V_{CL}^2)$ = static pressure coefficient
C_{P_0}	=	$(P_0 - P_{0CL})/(1/2\rho V_{CL}^2)$ = total pressure loss coefficient
H	=	δ^*/θ = boundary layer shape factor
K	=	$1 - \Gamma_{TV}/\Gamma_B$ = retained lift coefficient
L	=	lift force
P	=	static pressure
P_0	=	total pressure
r	=	radial co-ordinate
Re	=	$\rho V_{CL} c/\mu$ = Reynolds number based on blade chord
Re_d	=	$\rho V d/\mu$ = Reynolds number based on probe diameter
s	=	streamwise co-ordinate (Figure 4)
S	=	blade spacing
t	=	time
t_{MAX}	=	blade maximum thickness
u,v,w	=	components of velocity in the x, y and z directions
u'	=	root mean square velocity fluctuation in the x direction
v_θ	=	tangential component of velocity
V	=	resultant velocity
V_m	=	mean velocity through the cascade
x,y,z	=	co-ordinates in axial, tangential, and spanwise directions
x'	=	co-ordinate in chordwise direction
y'	=	local pitchwise co-ordinate (Fig. 2)
α	=	flow angle, measured from the axial direction
β	=	blade metal angle (Fig. 2)
γ	=	blade stagger angle (Fig. 2)
Γ_B	=	bound circulation
Γ_{TV}	=	circulation of the tip leakage vortex
Γ'	=	non-dimensional circulation (Γ/cV_1)
δ	=	boundary layer thickness
δ^*	=	$\int_0^\delta (1 - \frac{V}{V_e})\,dz$ = boundary layer displacement thickness

* Graduate Research Assistant.
** Associate Professor. Associate Member ASME.

Presented at the Gas Turbine and Aeroengine Congress and Exposition—June 4-8, 1989—Toronto, Ontario, Canada
This paper has been accepted for publication in the Transactions of the ASME
Discussion of it will be accepted at ASME Headquarters until September 30, 1989

θ	=	$\int_0^\delta (1 - \frac{V}{V_e}) \frac{V}{V_e} dz$ = boundary layer momentum thickness
Λ	=	Owen's eddy viscosity constant (Eqn. 9)
μ	=	viscosity
ν	=	kinematic viscosity (μ/ρ)
ν_e	=	eddy viscosity
ρ	=	density
σ	=	blade row solidity (c/S)
τ	=	tip gap
ω	=	vorticity
ω'	=	non-dimensional vorticity ($\omega c/V_1$)

Subscripts

cl	=	vortex centreline value
CL	=	undisturbed centreline value
e	=	boundary-layer edge value
min, max	=	minimum and maximum values
x,y,z,s	=	component in x, y, z and streamwise direction
1,2	=	cascade inlet, outlet

INTRODUCTION

The paper presents further experimental data from an on-going study of the tip-leakage flow in a planar cascade of turbine blades. Earlier papers have examined the effect of the leakage flow on the blade loading (Sjolander & Amrud, 1987) and the behaviour of the flow within the gap itself (Yaras et al., 1988). The data are quite extensive and are available in tabular form for use as a test case for computational methods (Yaras & Sjolander, 1988). The present paper focuses on the development of the vorticity field downstream of the trailing edge. The total pressure losses will be examined in a separate paper which is in preparation.

A knowledge of the strength and downstream evolution of the tip leakage vortex is useful in a number of ways. It gives insight into the losses since it appears that a significant fraction of the tip leakage losses occur through the diffusion, or mixing out, of the vortex. Also, it gives information about the cross flows which will be experienced at the inlet to a downstream blade row, and the influence of the axial blade spacing on the magnitude of these cross flows. The data are of course also useful for verifying the predictions of the modern, three-dimensional viscous flow calculation methods which are now being applied to blade passage flows with tip leakage (eg. Hah, 1986; Dawes, 1987).

The formation of the tip leakage vortex appears to have been documented first in the early 1950's through the measurements of and flow visualization of Dean (1954) and Rains (1954). Subsequently, Lakshminarayana & Horlock (1962, 1965) made extensive measurements of the leakage flow for an isolated compressor blade and a compressor cascade. Their studies revealed the structure of the vortex as it appears close to the trailing edge but they did not follow its development downstream. Later studies of the mean velocity and turbulence fields behind a compressor rotor (eg. Davino & Lakshminarayana, 1982; Pandya & Lakshminarayana, 1983a, 1983b) provide further information, although the vorticity again was not determined directly. Recently, Inoue and his co-workers have presented very detailed measurements of the flow field behind an axial compressor rotor (Inoue & Kuroumaru, 1984, 1988; Inoue et al., 1986). They did obtain the components of the vorticity vector and present the decay characteristics to a distance of 1.25 chord lengths downstream of the trailing edge. As evident, most previous studies of the tip leakage vortex have been conducted in compressor cascades and rotors.

It has been argued that not all of the bound circulation in the blade is shed downstream in the tip leakage vortex, unlike the case of a wing tip vortex. Instead, part of the vorticity is believed to jump the gap between the blade tip and the endwall in the form of a vortex sheet. This modified lifting-line model appears to have been suggested first by Lakshminarayana & Horlock (1962) and it subsequently formed the basis for Lakshminarayana's (1970) analysis of the tip vortex behaviour. The model is also used by Inoue and his co-workers to interpret their measurements. The modified lifting-line model implies that the fluid in the annulus between the tip and the endwall will effectively experience a lift force directly related to the circulation in the vortex sheet which crosses the gap. Values of this "retained lift" were obtained by Lakshminarayana & Horlock (1962, 1965) for an isolated compressor blade and compressor blades in cascade from pressures measured at the tip of the blade. Later, Lewis & Yeung (1977) measured the static pressure on the endwall above an isolated compressor blade using an array of taps which followed the blade contour. Based on these data, correlations for the retained lift as a function of clearance were proposed (see Figure 8). However, the correlations probably need further refinement to account for the effects of rotation.

If a broadly applicable correlation can be developed, the concept of retained lift appears useful since it provides a basis for estimating the circulation in the tip leakage flow from the blade lift, a known quantity. The data presented here are therefore examined and discussed partly in the context of this conceptual model.

As indicated, most previous studies of the downstream behaviour of the tip vortex have considered compressor flows. The present study broadens the scope of the available data by examining the behaviour of the tip leakage vortex in the higher-turning flow of an axial turbine. The experiment is of course still rather idealized. The effect of rotation, which acts in opposite directions on the gap flow in compressors and turbines, is not taken into account. Also, the flow was essentially incompressible and had a low level of freestream turbulence. Nevertheless, we feel that results give useful qualitative insights into some of the important aspects of the tip vortex behaviour in actual turbines.

EXPERIMENTAL APPARATUS AND PROCEDURES

Test Section and Test Cascade

The test section, which is shown schematically in Figure 1, has been described in detail in the earlier papers. The clearance is varied by using shims between the tip wall and the side walls. The side flaps and tailboards are used establish periodic flow within the cascade. The flow periodicity is determined from static pressure measurements on the endwall inside each blade passage and from measurements of the velocity vector at midspan downstream of the cascade. The periodicity is checked and adjusted for each clearance.

Figure 2 summarizes the geometry of the test cascade and shows the location of the downstream traverse planes. Measurements have been made at three main planes from the

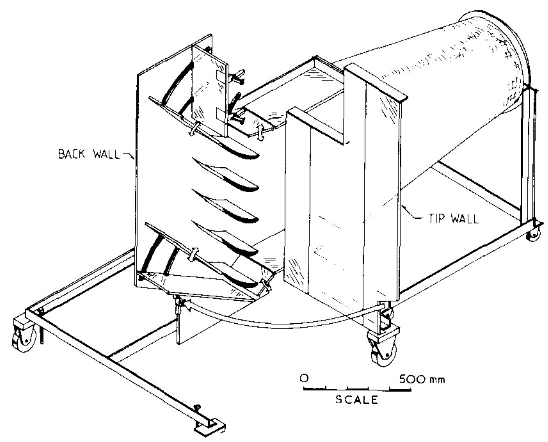

FIG. 1. CASCADE TEST SECTION

TABLE 1. TEST MATRIX AND INLET FLOW CONDITIONS.

			CLEARANCE (τ/c)			
		x/c_x	0.015	0.020	0.028	0.055
TRAVERSE PLANES	B	1.03	X	X	X	X
	C1	1.96	X	X	X	X
	C2	2.01	X	X	X	X
	D	2.56				X
τ (mm)			3.8	5.1	7.1	13.7
δ^*/τ			1.36	0.96	1.09	0.23
θ/τ			1.01	0.71	0.72	0.15
H			1.34	1.34	1.52	1.51

trailing edge to 1.56 axial chord lengths downstream. The probe can be moved easily to essentially any position in the x direction. This feature was used to obtain velocity measurements at two closely-spaced planes at main plane C. These data allow all the gradients in velocity, and hence the complete vorticity vector, to be determined. The combinations of clearance and downstream traverse planes which were examined are summarized in Table 1. As indicated, four clearances ranging from 1.5 to 5.5 percent of the blade chord were considered. The clearances heights were set to an estimated accuracy of ± 0.2 mm using feeler gauges.

In addition to the downstream flow field measurements, static pressures were measured on the blade surface and on the tip endwall. The middle blade in the cascade is instrumented with 14 rows of static taps extending from midspan to very close to the tip. Each row consists of 73 taps and thus gives a very detailed picture of the local

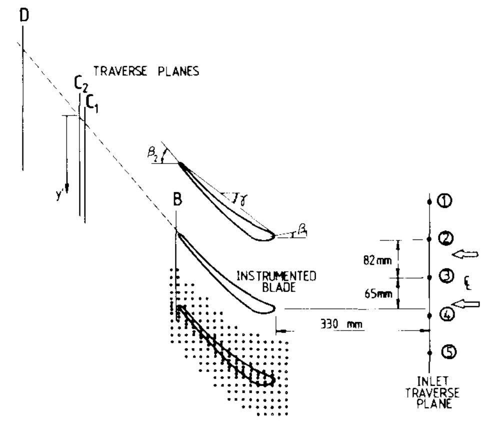

Chord Length, c	:	250 mm
Blade Thickness, t_{MAX}	:	24.6 mm
Blade Span, h	:	203 mm
Blade Spacing, S	:	150 mm
Aspect Ratio, h/c	:	0.812
Solidity, c/S	:	1.667
Stagger Angle, γ	:	37.2 ± 0.2 deg.
Blade Inlet Angle, β_1	:	11.1 ± 0.2 deg.
Blade Outlet Angle, β_2	:	49.6 ± 0.2 deg.

Fig. 2. SUMMARY OF CASCADE GEOMETRY.

loading on the blade. As indicated in Figure 2, the tip endwall is instrumented with a rectangular array of taps spanning one blade pitch.

Instrumentation

All pressures were measured using capacitive-type pressure transducers. The pressure signals were converted to digital form, with 12-bit resolution, using a Sciemetric Instruments data acquisition system which is controlled by an IBM PC-compatible microcomputer.

For the downstream traverses reported here, the flow field was measured using a conical, seven-hole pressure probe. The probe is mounted on a stem which projects through slots in the back wall of the test section. The stem attaches to a motorized traverse gear which allows the probe to be positioned at any point in a plane parallel to the trailing edges. It is estimated that the position of the probe is known to within ±0.25 mm in all three co-ordinate directions. The probe is aligned with the mean flow direction and then used in the non-nulling mode. This can lead to high angles of misalignment with the flow as the probe is traversed through the tip leakage vortex. The seven-hole probe was chosen since Everett et al. (1983) had indicated that this geometry is particularly suitable for high levels of flow misalignment, and our experience with the probe has been good. The probe is manufactured from seven tubes of equal diameter, which form a natural bundle, enclosed in a thin-walled outer tube. The interstices between the tubes are filled with solder and the measuring face is then machined to a conical or other suitable shape. Our probe has an outer diameter of 2.4 mm and the total cone angle of the face is 60 degrees. A small radius was applied to the mouth of the centre port to eliminate the sharp-edged shoulder at the tip of the probe.

As indicated, the probe was often severely misaligned with the flow. It was therefore calibrated, in steps of 5 degrees, through all combinations of pitch and yaw out to 50 degrees of misalignment for both angles. For measurements in flows where the resultant misalignment exceeds about 20 degrees, only data from the four ports on the windward side of the probe are used to obtain flow information. This avoids using pressures measured in the separated region on the leeward side where fluctuations are larger and the port pressure tends to be less sensitive to changes in the flow direction. Based on the scatter observed in the calibration measurements and other repeatability checks which were made, we estimate that in a reasonably uniform flow the angles inferred from the probe measurements would, conservatively, be accurate to within ±2 degrees and the total and dynamic pressures to within ±5 percent of the local dynamic pressure. In the cascade flow, the effect of strong shear and varying Reynolds number introduces some additional uncertainty.

There appears to be little information available on the effects of shear on five- and seven-hole pressure probes. In any event, it would be difficult to establish a laboratory flow with controlled levels of shear of the order of magnitude which we encounter in the tip leakage flow. Thus, we have no basis for applying corrections to our measurements or estimating the magnitude of the errors that may have been introduced. From internal checks on the data, we believe that our measurements have not been seriously compromised. For example, the values of circulation obtained for a given clearance at successive downstream planes are in good agreement, although as discussed later the slightly higher circulation detected at the trailing edge plane may be partly explained by measurement errors due to shear.

It is a common experience that the aerodynamic characteristics of conical five-hole pressure probes are quite sensitive to changes in Reynolds number. The seven-hole probe was calibrated at a probe Reynolds number, Re_d, of about 4100 corresponding roughly to the average value encountered in the downstream flow. In addition, representative calibration measurements were made for the complete range of Re_d seen in the cascade. When the calibration curves were applied to the data, flow angles were found to vary with Re_d by at most ±1.5 degrees and the inferred dynamic pressure by at most ±5.0 percent; for most combinations of pitch and yaw the errors were much smaller. Thus, our probe appears to be relatively insensitive to Re_d changes over the range we experience. This may be partly due to the rounding of the mouth of the centre port.

Determination of Vorticity

The components of the vorticity vector were obtained in Cartesian co-ordinates using a co-ordinate system aligned as shown in Figure 2:

$$\omega_x = \frac{\partial w}{\partial y} - \frac{\partial v}{\partial z}$$
$$\omega_y = \frac{\partial u}{\partial z} - \frac{\partial w}{\partial x} \qquad (1)$$
$$\omega_z = \frac{\partial v}{\partial x} - \frac{\partial u}{\partial y}$$

Thus the velocity gradients needed to determine ω_x can be obtained from flow field measurements made in a single plane parallel to the y-z plane. With some simplifying assumptions, approximate values of the other two components can also be obtained from such measurements. Assuming steady incompressible flow, neglecting the viscous terms, and substituting from (1), the momentum equation for the y direction can be rewritten as

$$\frac{1}{\rho}\frac{\partial P_0}{\partial y} + u\omega_z - w\omega_x = 0 \; . \qquad (2)$$

Solving for ω_z,

$$\omega_z = \frac{1}{u}\left[w\omega_x - \frac{1}{\rho}\frac{\partial P_0}{\partial y} \right] \qquad (3)$$

and all quantities on the right hand side of (3) are available from the measurements in the y-z plane. Similarly, from the momentum equation in the z direction:

$$\omega_y = \frac{1}{u}\left[\frac{1}{\rho}\frac{\partial P_0}{\partial z} + v\omega_x \right] \; . \qquad (4)$$

As a check on the accuracy of the values given by equations (3) and (4), flow field measurements were made, for each clearance, at two closely-spaced planes about one axial chord length downstream of the trailing edge. This allowed all the expressions in (1) to be evaluated directly. The agreement between the vorticity components obtained directly and the approximate values was excellent. The largest differences occurred near the edge of the vortex core where the velocity gradient is changing most rapidly and the viscous effects are therefore most important. However, even here the two values differed by less than 10 percent of the centreline vorticity, which is comparable with the uncertainty in either value. We intend to use only the approximate method in the future.

The flow field measurements downstream of the trailing edge were made on grids of evenly-spaced points extending one passage width and half the blade span. At the trailing edge, plane B, a grid spacing of 5 mm was used while at planes C1, C2, and D a spacing of 10 mm was found to be sufficient. All gradients in the y and z directions were obtained by central differences while the x-wise gradients determined from the measurements in planes C1 and C2 were calculated by simple differences. No smoothing was applied to the flow field data beyond the time-averaging performed during the data acquisition.

EXPERIMENTAL RESULTS

Operating Conditions

As in the earlier studies, all measurements were made for a Reynolds number of $4.3 \times 10^5 \pm 2$ percent, where the Reynolds number is based on the blade chord and undisturbed upstream velocity. The corresponding inlet velocity was about 30 m/s so that conditions were essentially incompressible. The freestream turbulence, u'/V_1, was about 1.5 percent at the inlet to the cascade for all cases. The integral parameters for the endwall boundary layer on the tip wall are given in Table 1. As the tip wall is moved outward to create the clearance, a ramp is inserted to provide the transition between the fixed upstream wall and the moveable section. This results in some variation in the boundary layer thickness with clearance. A similar trend was observed in the measurements reported by Yaras et al. (1988). As seen from the table, the displacement thickness of the tip wall boundary layer was roughly comparable with the smallest clearance.

The behaviour of the tip leakage vortex was found to be very similar for the four clearances. Therefore, detailed results will be presented only for 5.5 percent clearance, the case for which the most extensive measurements are available.

General Downstream Development of the Tip-Leakage Vortex

The general downstream development of the tip leakage vortex is shown in Figures 3a, 3b, and 3c which present contour plots of streamwise vorticity and total

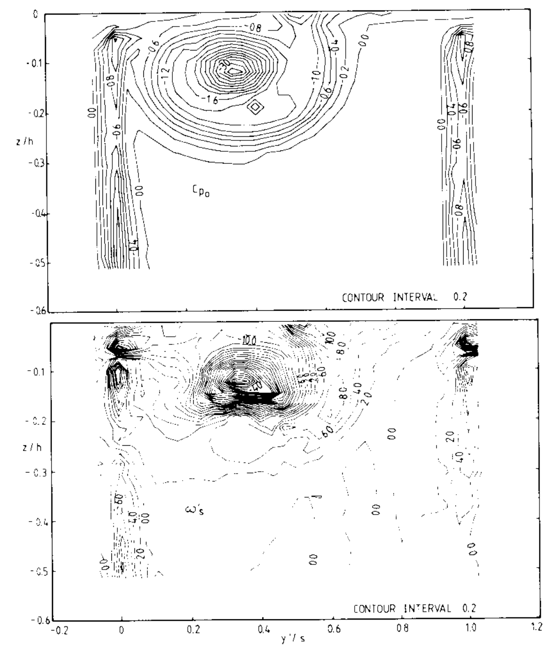

Fig. 3a. TOTAL PRESSURE AND STREAMWISE VORTICITY DISTRIBUTIONS (τ/c = 0.055, PLANE B).

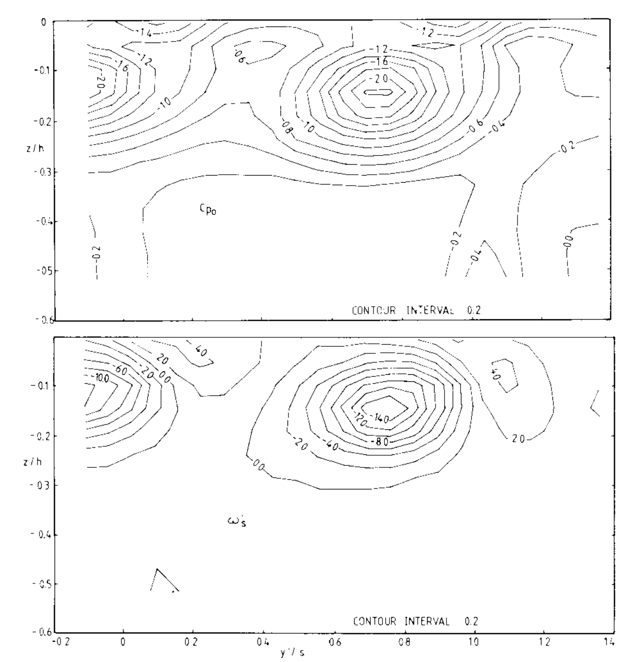

Fig. 3b. TOTAL PRESSURE AND STREAMWISE VORTICITY DISTRIBUTIONS (τ/c = 0.055, PLANE C2).

pressure loss at planes B, C2 and D for 5.5 percent clearance. The total pressure plots are included to indicate the position of the tip leakage vortex relative to the blade wakes; since the blades are two dimensional, comparatively little vorticity is shed in the wake and the wake is not very evident on the vorticity plots, except right at the trailing edge. The same contour interval was used on successive contour plots, to give a visual impression of the rapid diffusion of the tip vortex.

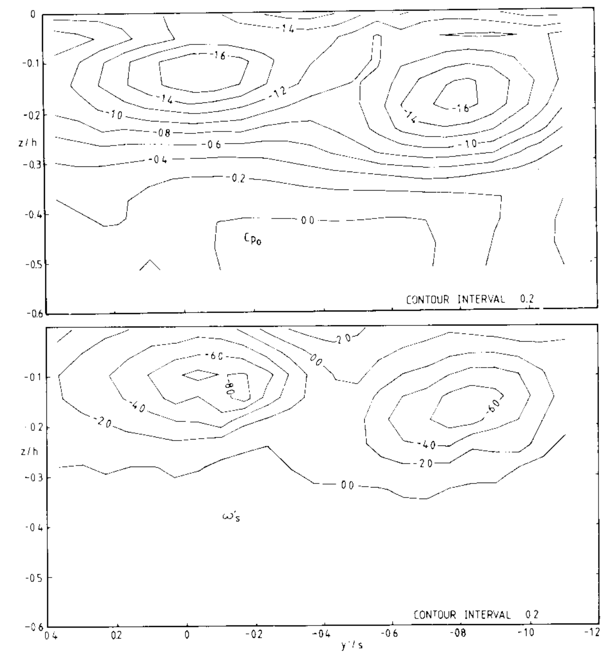

Fig. 3c. TOTAL PRESSURE AND STREAMWISE VORTICITY DISTRIBUTIONS (τ/c = 0.055, PLANE D).

Two vortices are evident from the plots for plane B. The tip vortex is clearly the dominant structure. However, at mid passage near the endwall there is also a small region of vorticity of the opposite sign which is probably the passage vortex. Sjolander and Amrud (1987) had found evidence from the blade pressure distributions of the formation of multiple tip leakage vortices at larger clearances. Such multiple vortices are not apparent from the present vorticity plots, suggesting that the vortices quickly interact to form a concentric resultant vortex, as might be expected from their proximity and the fact that their rotation is in the same direction.

The roll up of the tip vortex is clearly largely complete even at the trailing edge. Downstream of the trailing edge the vortex appears to migrate towards the pressure side of the passage flow. Inoue and his co-workers noted a similar behaviour for their compressor rotor flow. As seen from Figure 3b, at plane C2 the centreline of the vortex has moved three-quarters of the way across the passage flow and has begun to distort the next wake. The considerably smaller tip vortex for 2.0 percent clearance had moved to the middle of the passage flow by the time it reached plane C. For the largest clearance, it is clear that adjacent tip vortices are beginning to interact significantly by plane D, 1.56 axial chord lengths from the trailing edge.

As indicated in Figure 2, the traverse planes intersect the tip vortices at an oblique angle. When this angle was taken into account, it was in fact found that the tip vortex is quite close to being axisymmetric, even at the trailing edge. Therefore, the behaviour of other flow quantities will be presented only for a representative line passing through the centre of the vortex. The line parallel to the z axis was chosen since this line lies in the plane which is normal to the centreline of the vortex.

Simple Model for the Tip Leakage Vortex

The rapid roll-up and near axisymmetry of the tip vortex suggested that it might be possible to model the vortex approximately with a fairly simple model. Such a model would, for example, allow the designer to estimate at the preliminary design stage the cross-flows in the tip leakage vortex and their variation with downstream distance. Also, since the diffusion of the vortex is thought to contribute significantly to the total tip leakage loss, a simple vortex model might form a component of a semi-empirical method for estimating the losses.

The simplest starting point is the diffusion of a simple line vortex. For laminar flow and with the diffusion process beginning at time t = 0, the solution for the tangential velocity in the flow at any time t is (Lamb, 1932):

$$v_\theta = \frac{\Gamma}{2\pi r}\left[1 - e^{-\frac{r^2}{4\nu t}}\right] \tag{5}$$

and the radial distribution of the vorticity is given by

$$\omega_s = \frac{\Gamma}{4\pi\nu t}\, e^{-\frac{r^2}{4\nu t}} \quad . \tag{6}$$

Thus, the vorticity on the centreline (r = 0) is

$$\omega_{s_{cl}} = \frac{\Gamma}{4\pi\nu t} \quad . \tag{7}$$

This exact solution has been adapted, with some success, by Squire (1965) to provide a simple estimate for the diffusion with downstream distance of a turbulent wing-tip vortex. The vortex is assumed to start at some effective origin and then be convected downstream at the velocity of the surrounding stream, V. Then at any distance s from the origin, the local section of the vortex will have been diffusing laterally for a time t = (s/V). For the turbulent vortex, it is assumed that the turbulent momentum transport can be accounted for by a constant eddy viscosity, ν_e. Neglecting longitudinal mixing along the vortex, the solution for the turbulent vortex is then assumed to be given equations (4) and (5), with the viscosity replaced by $\nu_e + \nu$ and time replaced by (s/V). Squire suggested that the eddy viscosity should be a simple function of the circulation in the vortex:

$$\frac{\nu_e}{\nu} = a_s\left[\frac{\Gamma}{\nu}\right] \tag{8}$$

with a_s a constant. Γ/ν can be interpreted as the vortex Reynolds number. Subsequently, Owen (1970) developed a somewhat similar model but argued that the eddy viscosity should depend on the circulation according to

$$\frac{\nu_e}{\nu} = \Lambda^2\left[\frac{\Gamma}{\nu}\right]^{1/2} \tag{9}$$

with Λ a constant. Data from a variety of laboratory and flight experiments show that Λ varies from about 0.7 to 1.2 whereas a_s was found to vary over a range of nearly 10 (El-Ramly, 1972).

The simple line vortex model was applied to the tip leakage vortex using the nomenclature defined in Figure 4. The vortex is assumed to be convected downstream from its effective origin at $x = x_0$ at the downstream mean velocity, V_2. It is also assumed that the centreline of the vortex is aligned with V_2, and that the axial velocity is constant so that V_2 can be replaced by $V_1/\cos\alpha_2$. Then equation (7) can be written in terms of the geometric and flow parameters of the cascade flow as follows:

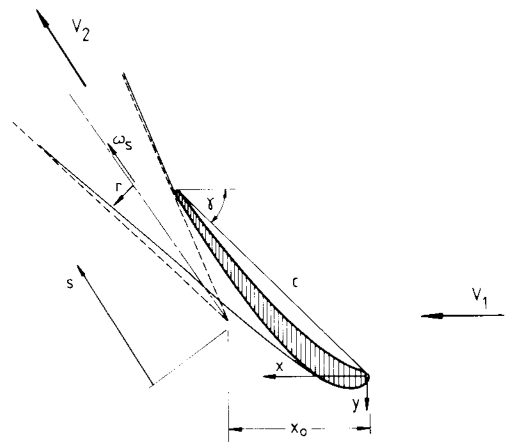

Fig. 4. TIP LEAKAGE VORTEX AS A DIFFUSING LINE VORTEX.

$$\omega_s{}' = \frac{\Gamma'}{4\pi}\;\frac{Re_c}{\left[\frac{\nu_e}{\nu}+1\right]\cos\gamma\left[\frac{x}{c_x}-\frac{x_o}{c_x}\right]} . \tag{10}$$

Using (10), experimental values of the eddy viscosity and the effective origin can be determined from the measured streamwise vorticity, on the centreline of the vortex, at two x-wise locations.

To apply the model, the designer would need to know the circulation of the tip leakage vortex, the eddy viscosity, and the axial position of the effective origin of the leakage vortex. Then from equation (5) the tangential velocity distribution through the vortex could be determined for any downstream position. The diffusion of the vortex as well as its diameter is completely defined for any position. The circulation for the tip vortex is examined next and correlations for the eddy viscosity and effective origin obtained for our cases are presented in later sections.

Retained Lift

As noted in the Introduction, Lakshminarayana & Horlock (1962) and Lewis & Yeung (1977) had suggested that only part of the blade's bound vorticity would be shed downstream in the tip leakage vortex. They inferred this from the effective blade loading at the endwall as obtained from static pressure measurements on the wall or from extrapolated blade surface pressures. The only direct measurements of the circulation in the tip leakage vortex, of which we are aware, are the data of Inoue et al. (1986) for a compressor rotor. They likewise found that for smaller clearances a fraction of the blade lift was "retained" at the endwall.

Indirect support for the concept of retained lift was presented by Yaras et al. (1988). Endwall static pressure measurements for clearances up to 3.2 percent showed that fluid near the endwall would experience a cross-channel pressure difference which was very similar to the undisturbed blade-to-blade pressure difference down inside the blade passage. These data are repeated on Figure 6 along with the

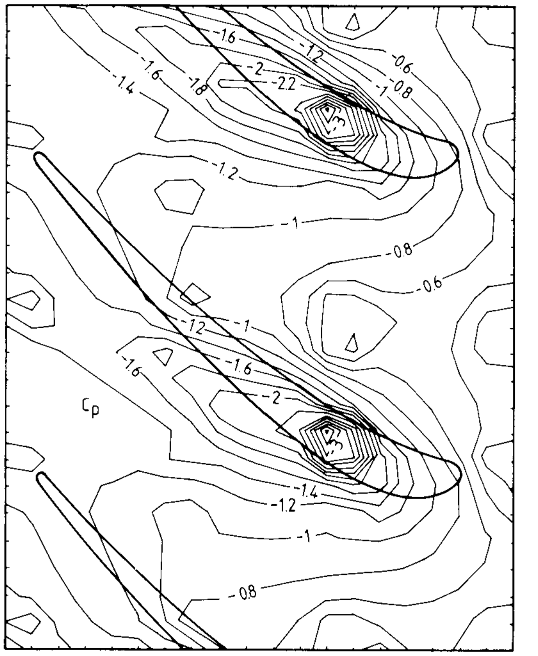

Fig. 5. STATIC PRESSURE DISTRIBUTION ON THE TIP ENDWALL (τ/c = 0.055).

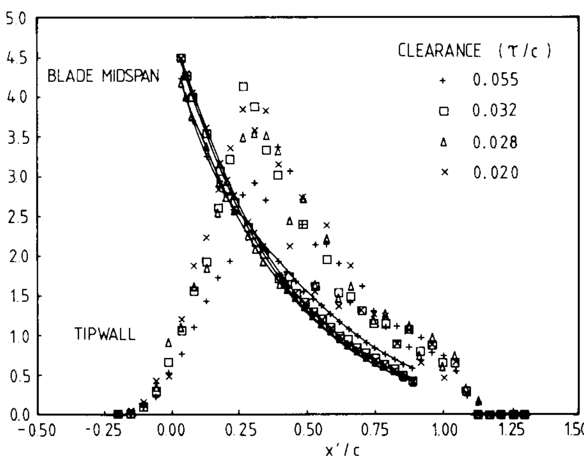

Fig. 6. COMPARISON BETWEEN BLADE MIDSPAN PRESSURES AND DRIVING PRESSURE DIFFERENCES AT ENDWALL.

new data for 5.5 percent clearance. The values of driving pressure difference in Figure 6 were obtained from contour plots such as Figure 5. The pressure coefficient at the blade suction peak is about -3.5. From Figure 5 it is seen that the minimum pressure coefficient on the endwall is about -3.0 for our largest clearance. There is thus beginning to be noticeable attenuation of the driving pressure near the endwall. This is further evident from Figure 6 which shows pressure differences on the endwall along lines which are approximately normal to the blade chord line and compares them with the blade midspan values. Although the pressure differences are reduced, it is nevertheless evident that fluid near the endwall will experience a significant cross-channel force, effectively a lift force, even for the 5.5 percent clearance.

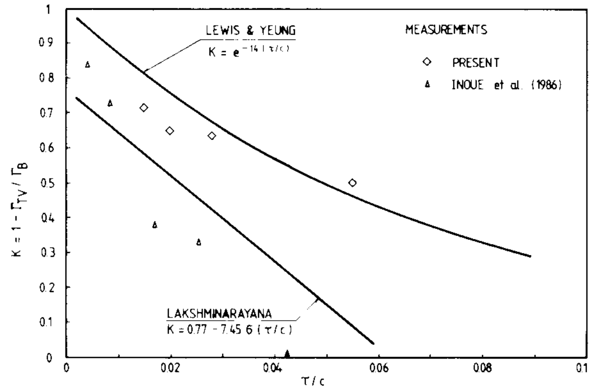

Fig. 7. VARIATION OF RETAINED LIFT COEFFICIENT WITH CLEARANCE.

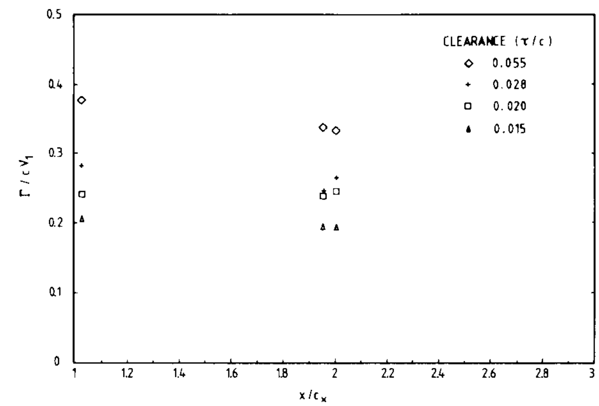

Fig. 8. VARIATION OF TIP VORTEX CIRCULATION WITH CLEARANCE AND DOWNSTREAM DISTANCE.

To quantify the retained lift effect, values of the shed and the bound circulation were obtained for each of the clearances. The circulation in the tip leakage vortex, Γ_{TV}, was obtained, from Stokes' Theorem, by integrating over the area the component of the vorticity normal to the traverse planes. The shed circulation was calculated for all traverse planes and the values for a given clearance were in good agreement, as shown in Figure 8. For present purposes, the average of the values obtained at planes C1 and C2 was used. The bound circulation was calculated from $\Gamma_B = L/\rho V_m$ where L is the lift obtained from the midspan blade pressures and V_m is the mean velocity through the blade row.

Figure 7 shows the measured variation of the retained lift coefficient, $K = 1 - \Gamma_{TV}/\Gamma_B$, with clearance for our experiment as well as for the compressor rotor experiment of Inoue et al. (1986). The correlations for retained lift proposed by Lakshminarayana & Horlock (1962) and Lewis & Yeung (1977) are also shown. As seen, our results are in reasonably good agreement with the correlation of Lewis & Yeung. However, it should be recalled that their correlation is based on lift values inferred from a ring of static taps which followed the blade profile on the endwall. As evident from Figure 5, such measurements for our flow would have led to much lower pressure differences than are in fact available to drive fluid either through the tip gap or across the passage. The agreement with Lewis & Yeung may therefore be somewhat fortuitous. In any event, it is clear that even for our largest clearance less than half the bound vorticity was shed downstream in the tip leakage vortex. For a given clearance, a much larger fraction of the bound vorticity was shed in the experiment of Inoue et al. This suggests that in

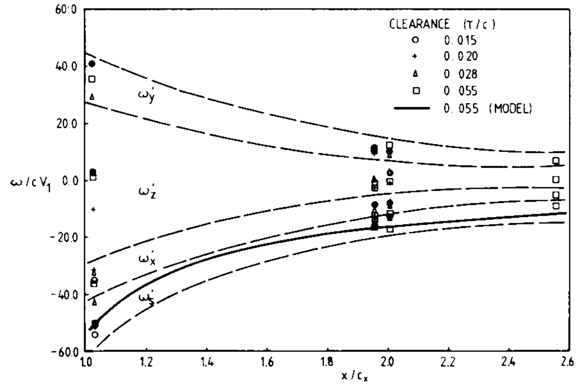

Fig. 9. VARIATION OF COMPONENTS OF VORTICITIY ON VORTEX CENTRELINE.

a compressor the rotation increases the vortex shedding as well as increasing the mass flow rate through the gap; the two effects are probably connected. It remains to be determined whether the reduced leakage mass flow rate which occurs in a turbine rotor also results in a weaker tip leakage vortex.

Downstream Variation of Circulation and Vorticity

Figure 8 shows the circulation for the tip leakage vortex as determined at planes B, C1 and C2 for each of the clearances. As seen, the values for a given clearance are in good agreement except that the value at the trailing edge plane tends to be a little higher. Physically, the circulation in the vortex could only be changing as a result of vorticity production or destruction at the endwall. Such production can in turn only be occurring if there is a pressure gradient at the wall. From Figure 5 it appears that endwall pressure gradients are very weak downstream of the trailing edge and the vorticity production should therefore be quite small. It seems likely therefore that the higher circulation obtained at plane B is mainly due to probe measurement errors arising from the effects of shear, which are strongest at this plane.

Figure 9 shows the variation of the three Cartesian components of vorticity as well as the streamwise component for the centreline of the vortex. To accommodate the growth of the vortex, its centreline should be inclined slightly relative to the endwall. Thus, one would expect a small negative component of vorticity in the z direction. As seen from the figure, the z component did tend to be negative. At main plane C, the values of ω_z were scattered over a range of about ± 3 non-dimensional vorticity units or about ± 20 percent of the centreline value of the streamwise vorticity. This probably gives a reasonable indication of the uncertainty present in all of the quoted vorticity values. Figure 9 shows that the tip leakage vorticity diffuses quite rapidly: the components on the centreline decline to about one quarter of their trailing edge value over the first axial chord length.

Figure 9 also shows the variation in the streamwise vorticity component for 5.5 percent clearance as calculated from the line vortex model. As discussed earlier, the model parameters are obtained from the measurements at two axial stations. The data from planes B and C were used here and thus only the comparison at plane D tests the models predictive capability. As seen, the predicted streamwise component agrees reasonably well with the measured value, bearing mind the uncertainty in the measurement. The ability of the model to predict the tangential velocity distribution through the vortex and the effective diameter of the vortex is examined in the next section.

To allow the vortex model to be applied to other blade rows, correlations must be developed for the eddy viscosity and effective origin of the vortex. Figure 10 summarizes the

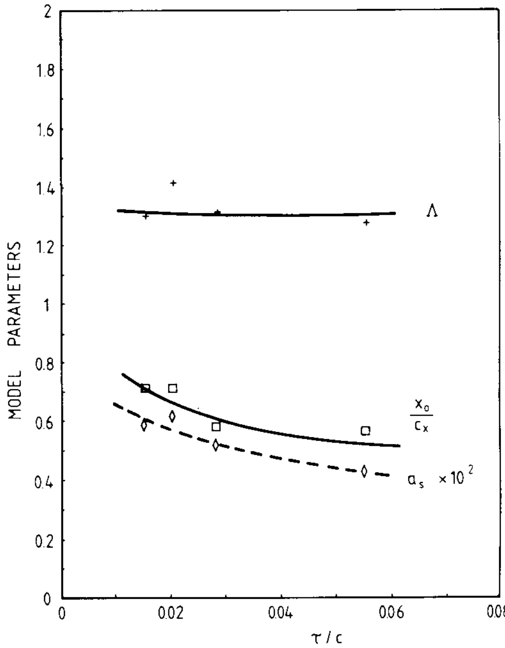

Fig. 10. VARIATION WITH CLEARANCE OF PARAMETERS FOR LINE VORTEX MODEL.

values of the parameters obtained here. As a matter of interest, the eddy viscosity was found to be about 500 to 650 times the molecular viscosity. As seen, Squire's eddy viscosity constant, a_s, decreases noticeably with increasing clearance. On the other hand, Owen's constant, Λ, seems to be scattered around a mean value of about 1.32. This is slightly above but close to the upper end of the range of Λ's observed in wing tip vortices. The results for the tip leakage vortex thus appear to support Owen's function (Eqn. 9) as a basis for obtaining the eddy viscosity, in agreement with the results for wing tip vortices. The effective origin of the tip vortex is seen to move forward with increasing clearance from about 72 percent of the chord length to about 55 percent for the range of clearances considered.

The correlation is of course incomplete in the sense that the important effects of rotation are not explicitly identified. The key to this may be the effect of the rotation on the shed circulation. The plot for the retained lift, Figure 7, gives an indication of the effect of rotation on the shed vorticity and thus on the tip-vortex Reynolds number, Γ_{TV}/ν. From equation (9), the eddy viscosity is simply a function of Γ_{TV}/ν and it would therefore implicitly vary with rotation. Likewise, it might be more appropriate to correlate the position of the effective origin with the vortex Reynolds number, rather than with the clearance as was done here. Additional data, for cases with actual or simulated rotation, are needed to confirm this.

Variation of Flow Parameters Through the Vortex

Finally, the variation through the vortex of a few selected parameters is presented.

Figure 11 shows the spanwise variation of the tangential component of velocity for 5.5 percent clearance. Also shown are the distributions calculated from the line vortex model. The results are presented with the vortex centres coincident; the relative position of the endwall is indicated. As seen, the measurements and the simple line vortex model are in surprisingly good agreement. Both indicate very strong cross-flows through the vortex at the trailing edge, plane B: the measured direction of the velocity

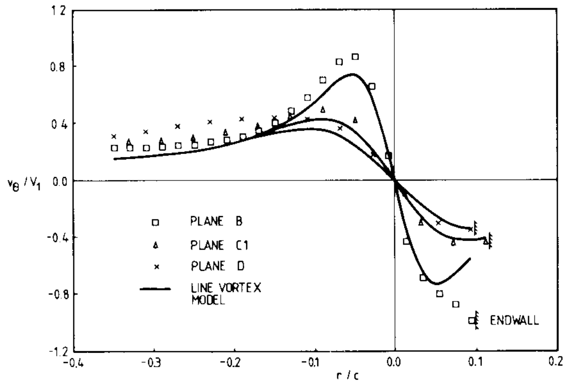

Fig. 11. SPANWISE DISTRIBUTION OF TANGENTIAL VELOCITY THROUGH CENTRE OF VORTEX (τ/c = 0.055).

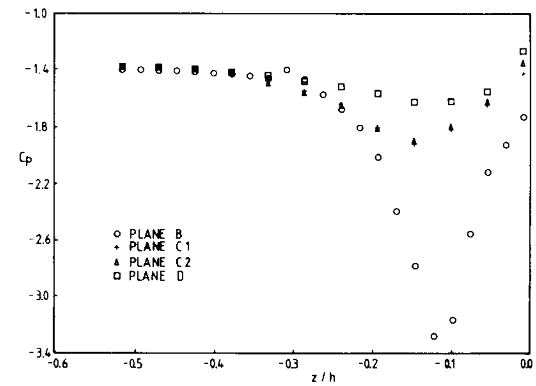

Fig. 12. SPANWISE STATIC PRESSURE DISTRIBUTION THROUGH CENTRE OF VORTEX (τ/c = 0.055).

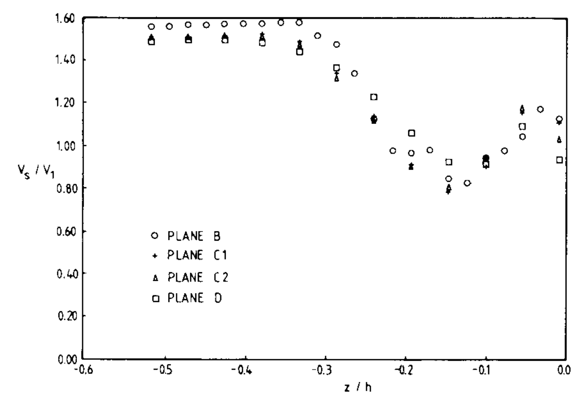

Fig. 13. SPANWISE DISTRIBUTION OF AXIAL VELOCITY THROUGH CENTRE OF VORTEX (τ/c = 0.055).

vector varied through a range of about 75 degrees, and the peak-to-peak variation through the model was only slightly smaller. Both show a core of nearly solid-body rotation and the core diameters, as indicated by the peaks in the crossflow velocity distributions, are also very similar. Both likewise show a similar decay in the crossflow velocities with downstream distance. The differences in the far field are explained by the fact that the velocities induced by the other tip vortices in the cascade are neglected in the model calculations. Their effect could easily be included.

The model assumes that all of the fluid in the vortex is convected downstream at the mean velocity of the surrounding stream. However, the diffusion of the actual vortex implies that there will be a rise in the static pressure along the its centreline. Figure 12 shows the static pressure distributions through the vortex as obtained from the seven-hole probe measurements. As shown, a very substantial rise does indeed occur. The static pressure rise also leads to relative flow up the centre on the vortex. Figure 13 shows that the axial velocity is in fact reduced by almost half at the centre of the vortex. The presence of this relative axial flow, which is neglected in the line vortex model, makes it even more remarkable that the simple model works as well as it does.

CONCLUSIONS

Detailed data have been obtained for the development of the tip leakage flow downstream of a turbine cascade. It was found that the circulation in the tip leakage vortex was substantially less than the bound circulation for the blade. Even at the largest clearance of 5.5 percent of the blade chord, the shed circulation was less than half the bound circulation. This supports Lakshminarayana and Horlock's modified lifting-line model which indicates that for a turbomachinery blade with clearance, part of the bound circulation can jump the tip gap in the form of a vortex sheet and only the balance is shed downstream. The tip vortex itself appeared to have essentially completed its roll-up by the time it reaches the trailing edge plane, and even here the structure was nearly axisymmetric. These characteristics make the tip leakage vortex amenable to a simple approximate analysis.

Although it only contains a fraction of the available circulation, the tip leakage vortex is nevertheless a powerful structure. At the trailing edge plane, it was found that the direction of the velocity vector varied by about 75 degrees through the vortex. On the other hand, the vortex diffuses rapidly with distance. Over the first axial chord length, the components of vorticity on the centreline were found to decrease by a factor of about four.

The present data are extensive and detailed and can thus be used as a test case for modern turbomachinery viscous flow prediction codes. In addition, it was shown that a very simple model based on the diffusion of a line vortex can be used to obtain reasonable estimates of the lateral diffusion of the line vortex, the crossflow velocities through it, and the growth of its diameter with downstream distance. Correlations are presented for the two parameters needed to calculate the vortex development, namely the location of its effective origin and the eddy viscosity in the vortex. Further data on the effects of rotation are needed to verify the general validity of the correlations.

ACKNOWLEDGMENTS

Financial support for this study provided by the Natural Sciences and Engineering Research Council of Canada under Grant A1671 and by Pratt & Whitney Canada Inc. is gratefully acknowledged.

REFERENCES

Davino, R.M., and Lakshminarayana, B., 1982, "Characteristics of Mean Velocity in the Tip Region of Turbomachinery Rotor Exit," AIAA Journal, Vol. 20, No. 4, April 1982, pp. 528-535.

Dawes, W.N., 1987, "A Numerical Analysis of the Three-Dimensional Viscous Flow in a Transonic Compressor Rotor and Comparison with Experiment," ASME Journal of Turbomachinery, Vol. 109, No. 1, January 1987, pp. 83-90.

Dean, R.C., 1954, "The Influence of Tip Clearance on Boundary- Layer Flow in a Rectilinear Cascade," M.I.T. Gas Turbine Laboratory, Report No. 27-3, 1954.

El-Ramly, Z., 1972, "Aircraft Trailing Vortices: A Survey of the Problem," Report No. ME/A 72-1, Carleton University, Ottawa, Canada, November 1972.

Everett, K.N., Gerner, A.A., and Durston, D.A., 1983, "Seven-Hole Cone Probes for High Angle Flow Measurement: Theory and Calibration," AIAA Journal, Vol. 21, No. 7, July 1983, pp. 992-998.

Hah, C., 1986, "A Numerical Modelling of Endwall and Tip Clearance Flow of an Isolated Compressor Rotor," ASME Journal of Engineering for Gas Turbines and Power, Vol. 108, No. 1, January 1986, pp. 15-21.

Inoue, M., and Kuroumaru, M., 1984, "Three-Dimensional Structure and Decay of Vortices Behind an Axial Flow Rotating Blade Row," ASME Journal of Engineering for Gas Turbines and Power, Vol. 106, No. 3, July 1984, pp. 561-569.

Inoue, M., and Kuroumaru, M., 1988, "Structure of Tip Clearance Flow in an Isolated Axial Compressor Rotor," ASME Paper 88-GT-251, to be published, ASME Transactions.

Inoue, M., Kuroumaru, M., and Fukuhara, M., 1986, "Behaviour of Tip Leakage Flow Behind an Axial Compressor Rotor," ASME Journal of Engineering for Gas Turbines and Power, Vol. 108, No. 1, January 1986, pp. 7-13.

Lakshminarayana, B., 1970, "Methods of Predicting the Tip Clearance Effects in Axial Flow Turbomachinery," ASME Journal of
Basic Engineering, Sept. 1970, pp. 467-480.

Lakshminarayana, B., 1986, "Tip Clearance Effects in Turbomachines," von Karman Institute/Pennsylvania State University Lecture Course on Tip Clearance Effects in Axial Turbomachines, April 1986.

Lakshminarayana, B. and Horlock, J.H., 1962, "Tip-Clearance Flow and Losses for an Isolated Compressor Blade," ARC R.& M. 3316.

Lamb, H., 1932, Hydrodynamics, 6th ed., Cambridge University Press, London, 1932.

Lewis, R.I., and Yeung, E.H.C., 1977, "Vortex Shedding Mechanisms in Relation to Tip Clearance Flows and Losses in Axial Fans," ARC R.& M. 3829.

Owen, P.R., 1970, "The Decay of a Turbulent Trailing Vortex," Aeronautical Quarterly, February 1970, pp. 69-78.

Pandya, A. and Lakshminarayana, B., 1983a, "Investigation of the Tip Clearance Flow Inside and at the Exit of a Compressor Rotor Passage - Part I: Mean Velocity Field," ASME Journal of Engineering for Power, Vol. 105, No. 1, January 1983, pp. 1-12.

Pandya, A. and Lakshminarayana, B., 1983b, "Investigation of the Tip Clearance Flow Inside and at the Exit of a Compressor Rotor Passage - Part II: Turbulence Properties," ASME Journal of Engineering for Power, Vol. 105, No. 1, January 1983, pp. 13-17.

Rains, D.A., 1954, "Tip Clearance Flows in Axial Flow Compressors and Pumps," Rept. No. 5, Hydrodynamics and Mechanical Engineering Laboratories, California Institute of Technology.

Sjolander, S.A., and Amrud, K.K., 1987, "Effects of Tip Clearance on Blade Loading in a Planar Cascade of Turbine Blades," ASME Journal of Turbomachinery, Vol. 109, pp. 237-244.

Squire, H.B., 1965, "The Growth of a Vortex in Turbulent Flow," Aeronautical Quarterly, August 1965, pp. 302-306.

Yaras, M., and Sjolander, S.A., 1988, "Measurements of the Tip Clearance Flow in a Rectilinear Cascade of Turbine Blades: A Test Case for Computational Methods," Tech. Rept. M&AE 88-1, Carleton University, Ottawa, Canada, April 1988.

Yaras, M., Zhu, Y., and Sjolander, S.A., 1988, "Flow Field in the Tip Gap of a Planar Cascade of Turbine Blades," ASME Paper 88-GT-29, accepted for ASME Transactions.